A Measurement of the K_S Lifetime

The NA48 Collaboration

A. Lai, D. Marras

Dipartimento di Fisica dell'Università e Sezione dell'INFN di Cagliari, I-09100 Cagliari, Italy.

J.R. Batley, A. Bevan[1], R.S. Dosanjh, T.J. Gershon[2], B. Hay[3], G.E. Kalmus, C. Lazzeroni, D.J. Munday, M.D. Needham[4], E. Olaiya, M.A. Parker, T.O. White, S.A. Wotton
Cavendish Laboratory, University of Cambridge, Cambridge, CB3 0HE, U.K.[5].

G. Barr, G. Bocquet, A. Ceccucci, T. Cuhadar-Dönszelmann, D. Cundy, G. D'Agostini, N. Doble, V. Falaleev, W. Funk, L. Gatignon, A. Gonidec, B. Gorini, G. Govi, P. Grafström, W. Kubischta, A. Lacourt, M. Lenti[6], S. Luitz[7], J.P. Matheys, I. Mikulec[8], A. Norton, S. Palestini, B. Panzer-Steindel, D. Schinzel, G. Tatishvili[9], H. Taureg, M. Velasco, O. Vossnack, H. Wahl
CERN, CH-1211 Genève 23, Switzerland.

C. Cheshkov, A. Gaponenko[10], P. Hristov, V. Kekelidze, D. Madigojine, N. Molokanova, Yu. Potrebenikov, A. Tkatchev, A. Zinchenko
Joint Institute for Nuclear Research, Dubna, Russian Federation.

I. Knowles, V. Martin, H. Parsons, R. Sacco, A. Walker
Department of Physics and Astronomy, University of Edinburgh, Edinburgh, EH9 3JZ, U.K.[5].

M. Contalbrigo, P. Dalpiaz, J. Duclos, P.L. Frabetti[11], A. Gianoli, M. Martini, F. Petrucci, M. Savrié, M. Scarpa
Dipartimento di Fisica dell'Università e Sezione dell'INFN di Ferrara, I-44100 Ferrara, Italy.

A. Bizzeti[12], M. Calvetti, G. Collazuol, G. Graziani, E. Iacopini, F. Martelli[13], M. Veltri[13]
Dipartimento di Fisica dell'Università e Sezione dell'INFN di Firenze, I-50125 Firenze, Italy.

H.G. Becker, H. Blümer, D. Coward, M. Eppard, H. Fox, A. Hirstius, K. Holtz, A. Kalter, K. Kleinknecht, U. Koch, L. Köpke, P. Lopes da Silva, P. Marouelli, I. Pellmann, A. Peters, S.A. Schmidt, V. Schönharting, Y. Schué, R. Wanke, A. Winhart, M. Wittgen
Institut für Physik, Universität Mainz, D-55099 Mainz, Germany[14].

J.C. Chollet, S. Crépé, L. Fayard, L. Iconomidou-Fayard, J. Ocariz, G. Unal,
I. Wingerter-Seez

*Laboratoire de l'Accélérateur Linéaire, IN2P3-CNRS,Université de Paris-Sud, 91898
Orsay, France*[15].

G. Anzivino, P. Cenci, E. Imbergamo, P. Lubrano, A. Mestvirishvili, A. Nappi, M. Pepe,
M. Piccini

*Dipartimento di Fisica dell'Università e Sezione dell'INFN di Perugia, I-06100 Perugia,
Italy.*

L. Bertanza, A. Bigi, P. Calafiura, R. Carosi, R. Casali, C. Cerri, M. Cirilli[16],
F. Costantini, R. Fantechi, S. Giudici, I. Mannelli, G. Pierazzini, M. Sozzi

*Dipartimento di Fisica, Scuola Normale Superiore e Sezione dell'INFN di Pisa, I-56100
Pisa, Italy.*

J.B. Cheze, J. Cogan, M. De Beer, P. Debu, F. Derue, A. Formica, R. Granier de
Cassagnac, E. Mazzucato, B. Peyaud, R. Turlay, B. Vallage

DSM/DAPNIA - CEA Saclay, F-91191 Gif-sur-Yvette, France.

I. Augustin, M. Bender, M. Holder, A. Maier, M. Ziolkowski

Fachbereich Physik, Universität Siegen, D-57068 Siegen, Germany[17].

R. Arcidiacono, C. Biino, N. Cartiglia, R. Guida, F. Marchetto, E. Menichetti,
N. Pastrone

*Dipartimento di Fisica Sperimentale dell'Università e Sezione dell'INFN di Torino,
I-10125 Torino, Italy.*

J. Nassalski, E. Rondio, M. Szleper, W. Wislicki, S. Wronka

*Soltan Institute for Nuclear Studies, Laboratory for High Energy Physics, PL-00-681
Warsaw, Poland*[18].

H. Dibon, G. Fischer, M. Jeitler, M. Markytan, G. Neuhofer, M. Pernicka, A. Taurok,
L. Widhalm

*Österreichische Akademie der Wissenschaften, Institut für Hochenergiephysik, A-1050
Wien, Austria*[19].

To be published in Physics Letters B

Abstract

A measurement of the K_S lifetime is presented using data recorded by the NA48
experiment at the CERN-SPS during 1998 and 1999. The K_S lifetime is derived from
the ratio of decay time distributions in simultaneous, collinear K_S and K_L beams,
giving a result which is approximately independent of the detector acceptance and
with reduced systematic errors. The result obtained is $\tau_S = (0.89598 \pm 0.00048 \pm
0.00051) \times 10^{-10}$ s, where the first error is statistical and the second systematic.

---

1   Introduction

Precise measurements of the basic physics parameters defining the neutral kaon system, such as the masses and mean lifetimes of the K_S and K_L states, are important not only in their own right but also as essential inputs to many kaon physics analyses such as studies of indirect and direct CP violation or precision tests of CPT invariance.

The K_S lifetime is presently known with a relative precision of about 0.1% [1], dominated by measurements from the NA31 experiment at CERN [2] and from the E731 and E773 experiments at Fermilab [3, 4]. Here we present a measurement of the K_S lifetime from the NA48 experiment at the CERN-SPS, based on the same $K^0 \to \pi\pi$ data samples as used for the precise determination of the direct CP violation parameter $\text{Re}(\epsilon'/\epsilon)$ [5]. The K_S lifetime is measured using an analysis technique introduced by NA31, namely a fit to the K_S/K_L ratio of decay time distributions reconstructed in nearly collinear K_S and K_L beams. This gives a result which is essentially independent of the detector acceptance and therefore with reduced systematic errors; the K_L beam is in effect used to determine the detection efficiency for K_S decays.

The analysis method is described in more detail in the next section, followed in Sections 3 and 4 by a brief summary of the main features of the NA48 experiment and of the reconstruction and selection of $K^0 \to \pi\pi$ decays; further details can be found in [5]. The fit used to extract the K_S lifetime is described in Section 5 and the estimation of the systematic errors on the fitted lifetime is considered in Section 6.

2   The Method

A defining principle of the NA48 experiment is the simultaneous recording of decays occurring within a common decay region traversed by two almost collinear beams of neutral kaons. The relative target positions for each beam, one far upstream of the decay region and the other much closer, ensure that kaon decays in the two beams are due dominantly to the K_L or to the K_S component, respectively. Assuming equal detection efficiencies for decays from the K_S and K_L beams, the ratio $R = N_S/N_L$ of decay rates observed in each beam as a function of the longitudinal position z can be expressed as

$$R(E_K, z) = A(E_K)\frac{f_S(t_S)}{f_L(t_L)} \qquad (1)$$

where E_K is the kaon energy, $A(E_K)$ is a normalisation function which depends on the relative beam intensities and $t_{S,L} = (z - z_{\text{targ S,L}})(m_K/p_K)$ are the proper lifetimes for kaon decays in the K_S or K_L beams. The functions $f(t)$ are given by

$$f_{S,L}(t) = e^{-t/\tau_S} + |\eta|^2 e^{-t/\tau_L} + 2D_{S,L}(E_K)|\eta|e^{-(t/\tau_S + t/\tau_L)/2}\cos\left(\Delta m \cdot t - \phi\right) \qquad (2)$$

where τ_S and τ_L are the K_S and K_L mean lifetimes, $\Delta m = m_L - m_S$ is the mass difference between the K_S and K_L states, $|\eta|$ and ϕ are the modulus and phase of the ratio $A(K_L \to \pi\pi)/A(K_S \to \pi\pi)$ of decay amplitudes, and the dilutions $D_{S,L}(E_K) = [N(K^0) - N(\overline{K}^0)]/[N(K^0) + N(\overline{K}^0)]$ reflect the initial admixture of K^0 and $\overline{K}^0$ in each beam. In practice, in place of z, it is convenient to analyse the longitudinal distribution of decay vertices in terms of the variable $\tau = (z - z_{\text{AKS}})(m_K/p_K)$ which measures the decay proper lifetime relative to the upstream edge of the decay region, defined by the position, z_{AKS}, of a set of scintillation counters.

Except for the K_L beam at higher energies, where the interference term contributes appreciably, the functions $f_S(t_S)$ and $f_L(t_L)$ are dominated by the exponential terms e^{-t_S/τ_S}

1

and $|\eta|^2 e^{-t_\mathrm{L}/\tau_\mathrm{L}}$, respectively. Hence the $\mathrm{K}_\mathrm{S}/\mathrm{K}_\mathrm{L}$ ratio is approximately of the form

$$R \propto \frac{e^{-t_\mathrm{S}/\tau_\mathrm{S}}}{e^{-t_\mathrm{L}/\tau_\mathrm{L}}} \propto e^{-\tau(1/\tau_\mathrm{S} - 1/\tau_\mathrm{L})} \ .$$

Since $\tau_\mathrm{L} \gg \tau_\mathrm{S}$, the ratio R is primarily sensitive to the K_S lifetime τ_S. The K_S lifetime is determined by fitting a function $R(E_\mathrm{K}, \tau)$ of the form given in Equations (1) and (2) to the ratio $N_\mathrm{S}/N_\mathrm{L}$ of $\mathrm{K}^0 \to \pi\pi$ decays reconstructed in the two beams. Besides the K_S lifetime itself, the normalisation $A(E_\mathrm{K})$ and the dilutions $D_\mathrm{S,L}(E_\mathrm{K})$ are also taken as free parameters in the fit, while the remaining physics parameters in equation (2) are taken from published measurements. Small acceptance differences between K_S and K_L decays are corrected using Monte Carlo, and background to the K_L samples is subtracted using the data. The $\pi^+\pi^-$ and $\pi^0\pi^0$ decay modes are analysed separately and the results subsequently combined.

The $\mathrm{K}_\mathrm{S}/\mathrm{K}_\mathrm{L}$ ratio is reconstructed in 20 bins of energy of width $\Delta E_\mathrm{K} = 5\,\mathrm{GeV}$ covering the range $70 < E_\mathrm{K} < 170\,\mathrm{GeV}$ and in lifetime bins of width $\Delta\tau = 0.1\tau_\mathrm{S}$. The fit to determine the K_S lifetime is carried out in the lifetime range $0.5\tau_\mathrm{S} < \tau < 3.5\tau_\mathrm{S}$. The lower lifetime limit of $0.5\tau_\mathrm{S}$ largely avoids detector resolution effects associated with the start of the decay region at $\tau = 0$ while the upper limit at $3.5\tau_\mathrm{S}$ is dictated by the trigger requirements. The choice of lifetime range approximately minimises the total error on the measured K_S lifetime.

3   The NA48 experiment

The K_L and K_S beams in the NA48 experiment are derived from $450\,\mathrm{GeV}$ protons incident on separate targets positioned $126\,\mathrm{m}$ and $6\,\mathrm{m}$ upstream of the decay region, respectively [6]. The K_S target is located $72\,\mathrm{mm}$ above the axis of the K_L beam. The K_S target and collimator system is aligned along an axis directed slightly downwards such that the K_S and K_L beams subtend an angle of $0.6\,\mathrm{mrad}$ and intersect at the centre of the detector, $120\,\mathrm{m}$ downstream of the K_S target.

The beginning of the decay volume is accurately defined by a K_S anti-counter (AKS) located at the exit of the K_S collimator. The AKS is composed of a photon convertor followed by three scintillator counters and is used to veto all upstream decays in the K_S beam. To minimise interactions of beam particles with air and material, the decay region itself is contained in a $90\,\mathrm{m}$ long evacuated tank terminated by a thin composite polyamide (Kevlar) window of $3 \times 10^{-3}\,X_0$ thickness. The tank is followed by the NA48 detector, the principal components of which are a magnetic spectrometer for charged particle detection, a liquid krypton calorimeter for photon and electron detection, an iron-scintillator hadron calorimeter, and muon counters consisting of three planes of scintillator shielded by $80\,\mathrm{cm}$ thick iron walls.

The charged particle spectrometer [7] consists of two drift chambers (DCH1 and DCH2) located before, and two drift chambers (DCH3 and DCH4) located after, a central dipole magnet. Each chamber has an area of $4.5\,\mathrm{m}^2$ and is made up of four sets of two staggered sense wire planes oriented along four directions (horizontal, vertical, $\pm 45°$). Track positions are reconstructed with a precision of $100\,\mu\mathrm{m}$ per view, while the momentum resolution is $\sigma(p)/p = 0.48\% \oplus 0.009 \times p(\mathrm{GeV}/c)\%$.

The liquid krypton calorimeter (LKr) [8] consists of ~ 13000 cells, each of cross section about $2\,\mathrm{cm} \times 2\,\mathrm{cm}$ and depth 27 radiation lengths. For the average photon energy of $25\,\mathrm{GeV}$, the transverse spatial resolution for photon showers is $1\,\mathrm{mm}$ and the energy resolution is 0.8%. The energy response is linear to about 0.1% in the range $5-100\,\mathrm{GeV}$.

The photon time resolution is $\sim 500\,\mathrm{ps}$ and the $\pi^0\pi^0$ event time is known with a precision of $\sim 220\,\mathrm{ps}$.

An evacuated beam pipe of radius $8\,\mathrm{cm}$ running along the full length of the detector on its central axis transports undecayed beam particles through each of the detector components. The beam tube and DCH drift chambers are aligned along the bisector of the converging $\mathrm{K_S}$ and $\mathrm{K_L}$ beams in order to equalise the acceptance for $\mathrm{K_S}$ and $\mathrm{K_L}$ decays. Undecayed neutral kaons in the $\mathrm{K_L}$ beam are largely confined within a transverse beam profile of radius $\sim 3.5\,\mathrm{cm}$ at the position of the NA48 detector. The $\mathrm{K_S}$ beam has a larger beam divergence and a correspondingly larger transverse profile of about $5\,\mathrm{cm}$ radius. Due to scattering in the beam collimators, both the $\mathrm{K_S}$ and $\mathrm{K_L}$ beams have an associated halo of particles extending to larger radii from the beam axis.

The trigger for $\pi^0\pi^0$ decays [9] requires that the total energy deposited in the LKr calorimeter be greater than $50\,\mathrm{GeV}$, that the kaon impact point at the calorimeter (had it not decayed) be within $15\,\mathrm{cm}$ of the beam axis, that the decay vertex be less than $5\ \mathrm{K_S}$ lifetimes from the beginning of the decay volume, and that each of the horizontal and vertical projections of the LKr energy distribution contain at most five peaks. The $\pi^0\pi^0$ trigger operates with negligible deadtime and high efficiency, $(99.920 \pm 0.009)\%$, with no significant difference between $\mathrm{K_S}$ and $\mathrm{K_L}$ decays. The first level of the $\pi^+\pi^-$ trigger [10] is based on signals from a scintillator hodoscope positioned in front of the LKr calorimeter and on the hit multiplicity in DCH1, and also requires a total energy in the LKr and hadron calorimeters of at least $35\,\mathrm{GeV}$. The second level trigger is based on tracks reconstructed using the information from DCH1, 2 and 4, and includes requirements that the decay vertex be less than $4.5\ \mathrm{K_S}$ lifetimes from the beginning of the decay volume and that the reconstructed mass be larger than $0.95\,m_\mathrm{K}$. The efficiency of the first and second level triggers is about 99.5% and 98.3%, respectively, again with no significant difference between $\mathrm{K_S}$ and $\mathrm{K_L}$ decays. The $\pi^+\pi^-$ trigger introduces a deadtime of about $1.1\,\%$.

4   Event Selection

$\mathrm{K^0} \rightarrow \pi\pi$ decays are reconstructed and selected using the same procedures and selection requirements as for the $\mathrm{Re}(\epsilon'/\epsilon)$ analysis [5]. The level of background remaining in the selected $\mathrm{K^0} \rightarrow \pi\pi$ samples, and the correction for acceptance differences between $\mathrm{K_S}$ and $\mathrm{K_L}$ decays, are also evaluated using similar techniques to those in [5]. For the determination of the $\mathrm{K_S}$ lifetime, it is the lifetime dependence of these corrections which is of importance, rather than their energy dependence or their overall normalisation.

4.1   The $\pi^0\pi^0$ sample

The reconstruction of $\pi^0\pi^0$ events is based entirely on data from the LKr calorimeter. Any group of four showers, each reconstructed within $5\,\mathrm{ns}$ of their average time, is considered. The energy of each shower is required to lie between 3 and $100\,\mathrm{GeV}$, and showers close to the edges of the calorimeter (within $11\,\mathrm{cm}$ of the outer edge or within $15\,\mathrm{cm}$ of the central axis) or within $2\,\mathrm{cm}$ of a defective cell are excluded. The transverse distance between any pair of showers must be greater than $10\,\mathrm{cm}$. The position of the centre of gravity of the event is defined as the energy-weighted average of the four shower positions. The radial distance, C_g, of the centre of gravity from the detector axis is required to be less than $10\,\mathrm{cm}$ to suppress events due to the decay of particles in the beam halo.

The kaon energy is estimated simply as the sum of the four shower energies. The longitudinal decay vertex position is reconstructed from the energies and positions of the

four showers, under the assumption that they come from the decay of a particle with the kaon mass, m_K, moving along the beam axis. A resolution of $\sim 40\text{-}60\,\mathrm{cm}$ is achieved on the vertex position, depending on the kaon energy and decay point. The shower pairing which best represents two $\pi^0 \to \gamma\gamma$ decays is inferred using a χ^2 variable constructed from the sum, $m_1 + m_2$, and difference, $m_1 - m_2$, of the two candidate $m_{\gamma\gamma}$ masses and a parameterisation of the resolutions on $m_1 \pm m_2$.

Background from $K_L \to \pi^0\pi^0\pi^0$ decays is suppressed by requiring no additional showers with energy greater than $1.5\,\mathrm{GeV}$ within $\pm 3\,\mathrm{ns}$ around the event time, and by requiring $\chi^2 < 13.5$ (which corresponds to 3.7σ on the $m_{\gamma\gamma}$ resolution). All other potential sources of background to the $\pi^0\pi^0$ sample are negligibly small.

The level of $K_L \to \pi^0\pi^0\pi^0$ background remaining in the $K_L \to \pi^0\pi^0$ sample is estimated using a control region at large values of χ^2, $36 < \chi^2 < 135$, dominated by background. Genuine $K_L \to \pi^0\pi^0$ signal events populating this control region are first subtracted using the $K_S \to \pi^0\pi^0$ data, for which background is negligible. Small differences in the shape of the χ^2 distribution for $K_S \to \pi^0\pi^0$ and $K_L \to \pi^0\pi^0$ decays are taken into account by applying a correction derived from Monte Carlo. The $K_L \to \pi^0\pi^0\pi^0$ background in the signal region, $\chi^2 < 13.5$, is estimated by extrapolating uniformly from the control region, with an additional factor $\lambda_{\mathrm{ext}} = 1.2 \pm 0.2$ derived from Monte Carlo simulation. The background estimation is carried out separately for each bin of kaon energy and proper lifetime. At low energy and at low lifetime, the fraction of $\pi^0\pi^0\pi^0$ background in the $\pi^0\pi^0$ sample is negligibly small, but rises with both energy and lifetime, reaching about $3\,\%$ for $E_K = 170\,\mathrm{GeV}$ and $\tau = 3.5\tau_S$. An increase of the background fraction with lifetime is to be expected since, when only four photons are detected in the LKr calorimeter, the reconstructed vertex position for a $K_L \to \pi^0\pi^0\pi^0$ decay is shifted downstream from its true position, while $K_L \to \pi^0\pi^0\pi^0$ decays occuring upstream of the decay region are largely removed by the K_L beam collimators.

4.2 The $\pi^+\pi^-$ sample

$K^0 \to \pi^+\pi^-$ events are reconstructed from oppositely charged pairs of tracks found in the magnetic spectrometer. Each track is required to have momentum greater than $10\,\mathrm{GeV}$ and to lie at least $12\,\mathrm{cm}$ from the centre of each DCH. Each track is also required to lie within the acceptance of the LKr calorimeter and the muon counters after extrapolation downstream. The momentum-weighted average of the track positions after extrapolation to the LKr calorimeter is used to define the position of the centre of gravity of the event. Its radial distance, C_g, from the detector axis is required to be less than $10\,\mathrm{cm}$.

The separation between the two tracks at their point of closest approach after extrapolation upstream from the spectrometer is required to be less than $3\,\mathrm{cm}$. The point midway between the tracks at their closest approach is used to define the decay vertex position. The resolution on the longitudinal position of the decay vertex is in the range $\sim 30\text{-}50\,\mathrm{cm}$, while the transverse resolution is about $2\,\mathrm{mm}$. The kaon momentum is computed from the opening angle θ of the two tracks and from the ratio p_+/p_- of their momenta, assuming that the event corresponds to a $K^0 \to \pi^+\pi^-$ decay. Thus the reconstruction of both the decay vertex position and the kaon momentum, and hence also of the proper time for the decay, depend only on the geometry of the detector.

Background to the $\pi^+\pi^-$ sample from $\Lambda \to p\pi^-$ decays is reduced to a negligible level by applying an energy dependent upper cut on the track momentum asymmetry $|p_+ - p_-|/(p_+ + p_-)$. This cut also serves to remove events with tracks at low radius to the beam axis in a way which depends only on the momentum ratio of the two tracks.

4

Background from $K_L \rightarrow \pi e \nu$ (K_{e3}) decays is suppressed by requiring E/p to be less than 0.8 for each track, while $K_L \rightarrow \pi \mu \nu$ ($K_{\mu3}$) decays are suppressed by rejecting events where one or both of the tracks is associated with a signal in the muon counters within ± 4 ns. Additional suppression of both K_{e3} and $K_{\mu3}$ decays is obtained by requiring that the $\pi^+\pi^-$ invariant mass, $m_{\pi\pi}$, be compatible with the kaon mass to within 3σ of the (energy-dependent) mass resolution, and by requiring a small missing transverse momentum, $p_T'^2 < 200 \, \mathrm{MeV}^2/c^2$, where p_T' is the component of the kaon momentum perpendicular to the line joining the production target (identified from the vertical position of the decay vertex, as described below) and the point where the kaon trajectory crosses the plane of the first drift chamber. The quantity p_T' has approximately the same resolution for $\pi^+\pi^-$ decays in both the K_S and K_L beams.

The level of background remaining in the $\pi^+\pi^-$ sample is estimated by extrapolating an exponential fitted to the $p_T'^2$ distribution in a control region, $800 < p_T'^2 < 2000 \, \mathrm{MeV}^2/c^2$, dominated by background, into the signal region $p_T'^2 < 200 \, \mathrm{MeV}^2/c^2$. Due to limited statistics, the lifetime bin width was increased from $0.1\tau_S$ to $0.5\tau_S$ for this procedure. The fraction of background in the $K_L \rightarrow \pi^+\pi^-$ sample is found to be about 2×10^{-3}, and no significant dependence of the background fraction on lifetime is observed in any bin of energy. An appreciable lifetime dependence is not expected in this case since both the signal and background are observed in the detector as two-track final states with configurations which vary in similar fashion with the decay vertex longitudinal position.

4.3 K_S tagging

For $\pi^+\pi^-$ decays, the good resolution on the transverse position of the decay vertex allows a clean separation of decays from the K_S and K_L beams; decays with a vertex position more than 4 cm above the K_L beam axis after extrapolation of the reconstructed parent kaon trajectory back to the position of the AKS counter were classed as belonging to the K_S beam ("vertex tagging"). For $\pi^0\pi^0$ decays, only the longitudinal position of the decay vertex can be reconstructed. In this case, the identification of decays from the K_S beam is accomplished using a tagging station (Tagger) traversed by the proton beam during transport to the K_S target and consisting of two scintillator ladders (one horizontal, one vertical) [11]. Each scintillator counter has a time resolution of ~ 140 ps, and a proton crosses at least two counters. A $\pi^0\pi^0$ decay is classed as belonging to the K_S beam if a signal is observed in the Tagger within ± 2 ns of the reconstructed event time. A small fraction, $\alpha_{SL}^{00} = (1.6 \pm 0.5) \times 10^{-4}$, of $K_S \rightarrow \pi^0\pi^0$ decays are mistagged as belonging to the K_L beam due to Tagger detection inefficiencies. A larger fraction, $\alpha_{LS}^{00} = (10.692 \pm 0.020)\%$, of $K_L \rightarrow \pi^0\pi^0$ decays are mistagged as belonging to the K_S beam due to accidental proton signals in the Tagger in time with the event. The values of α_{SL}^{00} and α_{LS}^{00} were inferred from studies of the mistagging fractions α_{SL}^{+-} and α_{LS}^{+-} for vertex tagged $\pi^+\pi^-$ decays, combined with studies of $K_L \rightarrow \pi^0\pi^0$ and $K_L \rightarrow \pi^0\pi^0\pi^0$ decays to determine the small differences in mistagging rates between charged and neutral modes.

4.4   Event samples

Applying the selection cuts above to the data recorded by NA48 during 1998 and 1999 yielded samples of 13.2M $K_S \rightarrow \pi^+\pi^-$, 12.2M $K_L \rightarrow \pi^+\pi^-$, 3.1M $K_S \rightarrow \pi^0\pi^0$ and 2.8M $K_L \rightarrow \pi^0\pi^0$ events with reconstructed lifetimes in the range $0.5 < \tau/\tau_S < 3.5$, where the number of $\pi^0\pi^0$ events has been corrected for K_S-K_L mistagging.

Samples of simulated $K^0 \rightarrow \pi\pi$ events corresponding to about 3-5 times the data statistics were also available for analysis. The Monte Carlo included a detailed modelling

of the K_S and K_L beams (including the K_S beam halo) and used the GEANT package [12] for particle tracking and the simulation of processes such as multiple scattering, photon conversion, and secondary interactions. Simulation of the LKr calorimeter response was based on a library of electromagnetic and hadronic showers generated using GEANT. The simulated events were passed through the same reconstruction and selection code as the data. Asymmetric non-Gaussian tails in photon shower energies due to hadron photoproduction in the liquid krypton, which arise in about 3×10^{-3} of cases, were modelled using a parameterisation which was applied to the reconstructed shower energies in the Monte Carlo events.

4.5 Acceptance correction

Since the K_S and K_L beams are almost collinear, and since K_S and K_L decays are recorded simultaneously using a common trigger, the acceptances for K_S and K_L decays as a function of energy and position are equal to good approximation, and the detector acceptance essentially cancels in the K_S/K_L ratio of lifetime distributions from the two beams. For the $\pi^+\pi^-$ decay mode, effects due to decay in flight of the charged pions also cancel in the K_S/K_L ratio.

Small acceptance differences arise due to the different divergences and transverse profiles of the K_S and K_L beams and the consequent differences in illumination of the detector. Also, the different definition of the upstream edge of the decay region for the two beams introduces large acceptance differences at low values of the reconstructed lifetime. The AKS veto requirement effectively represents a cut $\tau > 0$ on the true lifetime of decays in the K_S beam while the upstream acceptance for K_L decays extends smoothly into the region $\tau < 0$. This difference is clearly seen in Figure 1 where examples of the uncorrected reconstructed lifetime distributions for the K_S and K_L beams are plotted.

Acceptance differences for K_S and K_L decays were accounted for by dividing the K_S/K_L ratio observed in the data by the acceptance ratio predicted by the Monte Carlo. The acceptance correction also took detector resolution effects (smearing) into account by defining the K_S and K_L acceptances as the ratio of the number of simulated events passing the selection cuts in a bin of *reconstructed* energy and lifetime to the number of generated events in the corresponding bin defined using the *true* energy and lifetime.

Resolution induced acceptance differences due to the AKS veto requirement are largely eliminated by restricting the lifetime range considered to the region $\tau > 0.5\tau_S$. A small (up to $\sim 2\%$) residual variation of the acceptance correction remains for $\pi^0\pi^0$ events at low energy and lifetime, but the correction for $\pi^0\pi^0$ events is otherwise independent of lifetime within the errors due to Monte Carlo statistics. For $\pi^+\pi^-$ events, the K_S/K_L acceptance ratio is independent of lifetime at lower energies, but falls significantly (by up to $\sim 7\%$) with increasing lifetime at higher energies. This is not due to an intrinsic difference between the K_S and K_L acceptances, but rather to a slow decrease of the acceptance with increasing radial distance of the decay vertex from the beam axis, convoluted with the larger transverse size of the K_S beam. The fall in acceptance with increasing radius is due dominantly to the geometrical cuts and to the cut on the track momentum asymmetry, and can be reliably modelled and checked by comparing the relevant reconstructed distribution in data and Monte Carlo. Similarly, the modelling of the transverse beam profiles is checked by comparing the reconstructed C_g distributions in data and Monte Carlo.

6

5   Results

The K_S/K_L ratio $R = N_S/N_L$ is computed in two-dimensional bins of energy and lifetime of width $\Delta E_K = 5\,\text{GeV}$ and $\Delta\tau = 0.1\tau_S$, and corrected bin-by-bin for residual background in the $K_L \to \pi^+\pi^-$ and $K_L \to \pi^0\pi^0$ samples and for small differences in the K_S and K_L acceptances, as described above. For the $\pi^0\pi^0$ mode, the K_S/K_L ratio is also corrected for K_S-K_L mistagging. Examples of the dependence of the corrected K_S/K_L ratio on the reconstructed proper lifetime τ are shown in Figure 1. The shapes of the separate K_S and K_L lifetime distributions change appreciably with energy, due largely to changes in the lifetime dependences of the $\pi^+\pi^-$ and $\pi^0\pi^0$ acceptances, but the corrected K_S/K_L ratio is approximately independent of energy.

The K_S lifetime is determined by fitting a function of the form given in Equations (1) and (2) to the K_S/K_L ratio over the lifetime range $0.5 < \tau/\tau_S < 3.5$ and energy range $70 < E_K < 170\,\text{GeV}$. The following χ^2 quantity is minimised in the fit:

$$\chi^2 = \sum_{i=1}^{20} \sum_{j=1}^{30} \left(\frac{R_{ij} - R(E_i, \tau_j)}{\sigma_{ij}} \right)^2$$

where E_i is the central energy of the i'th bin of energy, τ_j is the central value of the j'th bin of proper lifetime, R_{ij} is the corrected K_S/K_L ratio from the data, σ_{ij} is the statistical error on R_{ij}, and $R(E_i, \tau_j) = A_i f_S(t_S)/f_L(t_L)$ is the expected K_S/K_L ratio. The normalisation parameters $A_i = A(E_i)$ are allowed to vary in the fit. At low energies, $70 < E_K < 140\,\text{GeV}$, the values of the dilutions $D_S(E_K)$ and $D_L(E_K)$ appearing in the interference terms in the functions $f_S(t_S)$ and $f_L(t_L)$ are fixed using measurements of the dilution by the NA31 experiment [13]. The dilutions $D_S(E_K)$ and $D_L(E_K)$ rise from about 0.2 at $E_K = 70\,\text{GeV}$ to about 0.35 at $E_K = 140\,\text{GeV}$ and differ slightly because of the different kaon production angles (4.2 mrad and 2.4 mrad) used to define the K_S and K_L beams; small corrections are applied to the NA31 measurements to account for the different production angles used in this experiment. At high energies, $140 < E_K < 170\,\text{GeV}$, where the interference term contributes significantly to the ratio $R(E_K, \tau)$, the values $D_i = D_S(E_i) = D_L(E_i)$ of the dilution are allowed to vary in the fit, neglecting the small differences between the K_S and K_L dilutions. The remaining physics parameters appearing in the functions $f(t)$ are taken from the PDG averages of existing published measurements, except the K_S lifetime τ_S which is a free parameter in the fit.

The fit was carried out separately for the $\pi^+\pi^-$ and $\pi^0\pi^0$ samples from each year of data taking. The values of the K_S lifetime from each fit are summarised in Table 1. The errors are statistical only and include the contribution from finite Monte Carlo statistics. The minimum value of the fit χ^2 is also given in Table 1 and corresponds in all cases to an acceptable fit probability. Examples of the fit results and the fit quality for the $\pi^+\pi^-$ and $\pi^0\pi^0$ data samples from the 1999 run are shown in Figure 1. The effect of the interference terms in the fit function is visible in the plots for the high energy bin as a slight curvature of the lines representing the fit result.

Consistent values of the fitted K_S lifetime τ_S, and of the fitted normalisation and dilution parameters A_i and D_i, were found for the charged and neutral modes and for the samples from the different years of data taking. The fitted values of the dilution D_i within the energy range $140 < E_K < 170\,\text{GeV}$ were also consistent with the published NA31 measurements.
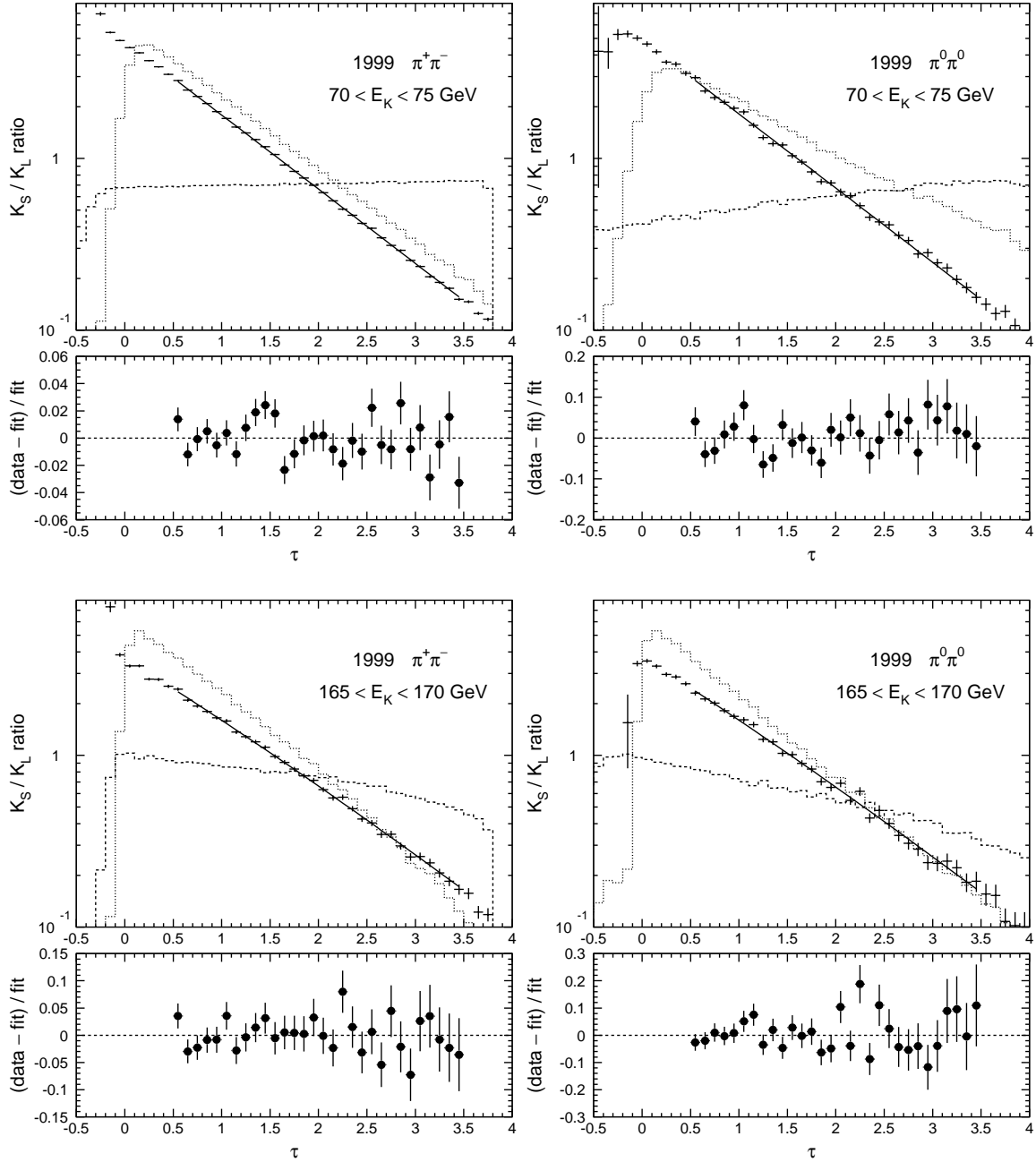
Figure 1: The points with error bars in the upper plot of each pair show examples of the corrected K_S/K_L ratio as a function of the reconstructed proper lifetime, τ, expressed in nominal K_S lifetime units of 0.8927×10^{-10} s. The dotted and dashed histograms show the corresponding uncorrected lifetime distributions for the K_S and K_L beams, arbitrarily normalised. The curves show the results of the fit for the K_S lifetime, while the lower plot of each pair shows the normalised fit residuals.

	$\pi^+\pi^-$		$\pi^0\pi^0$	
	$\tau_{\mathrm{S}}/10^{-10}\,\mathrm{s}$	χ^2/dof	$\tau_{\mathrm{S}}/10^{-10}\,\mathrm{s}$	χ^2/dof
1998	0.89578 ± 0.00109	$628.2/573$	0.89606 ± 0.00247	$551.0/573$
1999	0.89598 ± 0.00072	$601.2/573$	0.89635 ± 0.00167	$543.5/573$

Table 1: Values of the K_S mean lifetime and the minimum chi-squared per degree of freedom from the lifetime fits. The errors are statistical only.

6   Systematic errors

Various sources of systematic error on the measured K_S lifetime were considered, including uncertainties in the reconstruction of the energy and distance scales for the charged and neutral decay modes, and uncertainties due to the background subtraction, the tagging correction, the Monte Carlo acceptance correction, and the external physics parameters used in the fitting function.

As noted in Section 4.2, the energy and distance scales for reconstructed $\pi^+\pi^-$ events are determined largely by the detector geometry, especially of DCH1 and DCH2. The systematic error due to uncertainties in detector geometry was estimated by considering a variation of $\pm 2\,\mathrm{mm}$ in the longitudinal separation of DCH1 and DCH2 and a variation of $\pm 20\,\mu\mathrm{m/m}$ in the relative transverse scale of the two chambers. The position of the upstream edge of the $K_S \to \pi^+\pi^-$ decay vertex distribution was found to be consistent within these tolerances with the nominal position of the AKS counter. In addition, the momentum scale for reconstructed tracks was varied by $\pm 0.1\%$, as determined from the consistency of the reconstructed $\pi^+\pi^-$ invariant mass with the kaon mass, m_{K}. In each case, the kaon decay reconstruction was redone for all events in the data using the modified track positions or momenta, and the lifetime analysis repeated. The resulting change in the fitted K_S lifetime was taken as the estimate of the corresponding systematic error.

The systematic error due to uncertainties in the reconstruction of $\pi^0\pi^0$ events was estimated by varying the energy scale of reconstructed showers by $\pm 0.03\%$ and by varying the linearity and uniformity of the calorimeter response by modifying the reconstructed shower energy by an amount $\Delta E = \alpha + \beta E^2 + \gamma r E$, where r is the radial distance of the shower from the central detector axis. The allowed variation in the neutral energy scale is determined from a comparison of the position of the edge of the $K_S \to \pi^0\pi^0$ decay vertex distribution with the nominal position of the AKS counter. The allowed ranges of the constants α, β and γ are determined from studies of K_{e3}, $K^0 \to \pi^0\pi^0$ and $K_L \to \pi^0\pi^0\pi^0$ decays, and of $\pi^0 \to \gamma\gamma$ and $\eta \to \gamma\gamma$ decays in special runs with π^- beams.

The uncertainty due to the $K_L \to \pi^+\pi^-$ background subtraction was assessed by conservatively assigning a systematic error equal to $\pm 100\%$ of the change in the fitted K_S lifetime when the background subtraction was removed. The systematic error associated with the $K_L \to \pi^0\pi^0$ background subtraction was estimated by varying the extrapolation factor λ_{ext} within the range $\lambda_{\mathrm{ext}} = 1.2 \pm 0.2$.

The $K_L \to \pi^+\pi^-$ and $K_L \to \pi^0\pi^0$ samples contain a small fraction of events arising from the genuine $\pi\pi$ decay of neutral kaons produced by scattering in (dominantly) the final collimator of the K_L beam. In the charged mode, collimator scattered events are largely removed by the cut on $p_{\mathrm{T}}'^2$ and contribute a fraction less than 10^{-4} to the $K_L \to \pi^+\pi^-$ sample. This contribution is already included in the charged background estimate described in Section 4.2, and no additional systematic error is warranted. Studies of events with large transverse momentum ($p_{\mathrm{T}}'^2 > 200\,\mathrm{MeV}^2/c^2$) showed that the lifetime

Source	Variation	$\pi^+\pi^-$	$\pi^0\pi^0$	$\pi\pi$
DCH1 radial scale	$\pm 20\,\mu\text{m/m}$	± 1.8		± 1.5
DCH1 z position	$\pm 2\,\text{mm}$	± 0.2		± 0.1
Momentum scale	± 0.001	± 0.3		± 0.3
LKr Energy scale	± 0.0003		± 1.7	± 0.3
Energy loss (α)	$\pm 10\,\text{MeV}$		± 3.4	± 0.6
Non-linearity (β)	$\pm 0.00002\,\text{GeV}^{-1}$		± 1.6	± 0.3
Non-uniformity (γ)	$\pm 0.00001\,\text{cm}^{-1}$		± 1.0	± 0.2
LKr radial scale	± 0.0003		± 3.0	± 0.5
Charged background	$\pm 100\,\%$	± 1.4		± 1.2
Neutral background	$\lambda_\text{ext} = 1.2 \pm 0.2$		± 2.1	± 0.3
Collimator scattering	$\pm 100\,\%$		± 3.2	± 0.5
MC: K_S beam y posn	$\pm 2\,\text{mm}$	± 1.6	± 0.2	± 1.3
MC: K_L beam y posn	$\pm 2\,\text{mm}$	± 1.4	± 0.2	± 1.2
MC: K_S beam halo	$\pm 100\,\%$	± 1.3	± 1.3	± 1.4
MC: non-Gaussian tails	$\pm 50\,\%$		± 4.4	± 0.7
MC: statistics		± 3.0	± 4.9	± 2.7
τ_L	$5.17 \pm 0.04 \times 10^{-8}\,\text{s}$	± 0.1	± 0.1	± 0.1
$|\eta_{+-}|$, $|\eta_{00}|$	$2.276, 2.262 \pm 0.017 \times 10^{-3}$	± 0.1	± 0.1	± 0.1
ϕ_{+-}, ϕ_{00}	$43.3 \pm 0.5°, 43.2 \pm 1.0°$	± 0.8	± 0.4	± 0.8
Δm	$0.5300 \pm 0.0012 \times 10^{10}\,\text{s}^{-1}$	± 0.5	± 0.7	± 0.5
$D(E_\text{K})$	$\pm 2\,\sigma$	± 0.3	± 1.0	± 0.4
α_LS^{00}	0.10692 ± 0.00020		± 2.1	± 0.4
α_SL^{00}	$(1.6 \pm 0.5) \times 10^{-4}$		± 0.4	± 0.1
Fit method		± 2.7	± 2.7	± 2.7
Total systematic error		± 5.4	± 10.9	± 5.1
Statistical error		± 5.2	± 12.9	± 4.8

Table 2: Summary of systematic errors on the measured K_S lifetime, in units of $10^{-14}\,\text{s}$. The final column corresponds to a combination of the $\pi^+\pi^-$ and $\pi^0\pi^0$ results.

distribution of collimator scattered events corresponds approximately to an exponential decay characterised by the K_S, rather than K_L, lifetime, and that their energy distribution is similar to that of unscattered K_L decays. The high $p_\text{T}'^2$ events were also used to estimate the fraction, $(4.2 \pm 1.0) \times 10^{-4}$ [14], of collimator scattered events in the $\text{K}_\text{L} \to \pi^0\pi^0$ sample, where no transverse momentum cut is possible. For the $\pi^0\pi^0$ mode, the effect of collimator scattering on the K_S lifetime measurement was studied by modifying the fit function to be of the form $R(E_i, \tau_j) = A_i f_\text{S}(t_\text{S})/[f_\text{L}(t_\text{L}) + A_\text{coll} e^{-t_\text{coll}/\tau_\text{S}}]$ where $t_\text{coll} = (z - z_\text{coll})(m_\text{K}/p_\text{K})$ is the proper lifetime of the decay relative to the position of the final K_L collimator and A_coll is a constant which is adjusted to give the above fraction of collimator scattered events in the $\text{K}_\text{L} \to \pi^0\pi^0$ sample. This fraction was assumed to be independent of energy. The resulting systematic error was conservatively estimated as $\pm 100\%$ of the change in the K_S lifetime due to inclusion of the collimator scattering component in the fit.

The systematic error associated with uncertainties in the acceptance correction was estimated by varying the assumed vertical position of the K_S and K_L beams in the Monte Carlo within a range $\pm 2\,\text{mm}$ around their nominal positions. In addition, the sensitivity to the transverse beam profile was studied by switching off the simulation of the K_S beam

halo in the Monte Carlo. In each case, the resulting change in the fitted K_S lifetime was taken as the systematic error. The sensitivity of the acceptance correction to the modelling of the detector resolution was assessed by removing the simulation of non-Gaussian tails from the reconstructed photon shower energies, and a systematic error of $\pm 50\%$ of the effect on the fitted K_S lifetime was assigned. The effect of possible non-Gaussian tails in the reconstructed drift chamber hit positions was also studied in the Monte Carlo, but found to have a negligible effect on the fitted K_S lifetime. Finally, the component of the overall statistical error on the fitted lifetime arising from the finite Monte Carlo statistics was extracted, and classified as a separate systematic error.

The external physics parameters τ_L, η_{+-}, η_{00}, ϕ_{+-}, ϕ_{00} and Δm appearing in the functions $f(t)$ were each varied in turn within a range given by the error on the PDG average value. The mistagging fractions α_{LS}^{00} and α_{SL}^{00} were varied within the uncertainties given in Section 4.3. The value of the dilutions $D_{S,L}(E_K)$ in the energy range $70 < E_K < 140\,\text{GeV}$ was varied by twice the error on the NA31 measurements [13]. The extra factor of two conservatively takes into account uncertainties in correcting the NA31 measurements to the NA48 experiment.

The fitting procedure itself was tested by applying the fit to the generated inclusive energy and lifetime distributions of parent kaons from the Monte Carlo samples. No significant bias was observed on the fitted K_S lifetime, and the statistical precision of the test was assigned as a systematic error.

The systematic errors on the K_S lifetime from each of the above sources for the 1998 and 1999 data combined are summarised in Table 2. For comparison, the effect of the background subtraction is to increase the fitted K_S lifetime for the $\pi^0\pi^0$ mode by $12.8 \times 10^{-14}\,\text{s}$, while the acceptance correction from the Monte Carlo changes the K_S lifetime by $+22.5 \times 10^{-14}\,\text{s}$ and $-9.1 \times 10^{-14}\,\text{s}$ for the $\pi^+\pi^-$ and $\pi^0\pi^0$ modes, respectively.

The analyses carried out for each year of data taking and for each decay mode are combined taking into account any correlations between the separate analyses. The total systematic error is obtained by summing the individual errors in quadrature. The measured values of the K_S lifetime for each decay mode and for the two decay modes combined are:

$$\tau_S = (0.89592 \pm 0.00052 \pm 0.00054) \times 10^{-10}\,\text{s} \qquad (\pi^+\pi^-)$$
$$\tau_S = (0.89626 \pm 0.00129 \pm 0.00100) \times 10^{-10}\,\text{s} \qquad (\pi^0\pi^0)$$
$$\tau_S = (0.89598 \pm 0.00048 \pm 0.00051) \times 10^{-10}\,\text{s} \qquad (\pi^+\pi^- + \pi^0\pi^0)$$

where the first error is statistical and the second systematic.

Various cross-checks were performed to verify the integrity and stability of the result. No significant dependence of the fitted K_S lifetime was found on the lifetime or energy range used in the fit, or on the energy range within which $D(E_K)$ was allowed to vary in the fit. The effect of varying the main selection cuts used in the analysis was also studied, namely the cuts on $p_T'^2$, C_g, the momentum asymmetry $|p_+ - p_-|/(p_+ + p_-)$, and the minimum radii of tracks and clusters in DCH1 and the LKr calorimeter. In each case, either no statistically significant variation in the fitted lifetime was found, or the observed variation was found to be within the systematic errors assigned. The stability of the analysis was also tested by dividing the $\pi^+\pi^-$ data sample into topologies for which the positive and negative tracks initially curve towards or away from each other in the spectrometer magnetic field; consistent values of the fitted lifetime were found for the two topologies. Similarly, selecting either of the two polarities of the spectrometer magnetic

field setting gave consistent results. Other tests involved dividing the data samples according to the primary data-taking periods, the event time within the SPS spill, and the azimuthal orientation of the decay. For the charged mode, separating K_S and K_L decays using the Tagger in place of vertex tagging gave no significant change in the result.

7   Summary

The K_S lifetime has been measured using $K_S \to \pi\pi$ and $K_L \to \pi\pi$ decays recorded by the NA48 experiment in 1998 and 1999. The combined result for the $\pi^+\pi^-$ and $\pi^0\pi^0$ decay modes, $\tau_S = (0.89598 \pm 0.00048 \pm 0.00051) \times 10^{-10}$ s, has a precision better than that of the current PDG average [1] of existing measurements, and lies about 1.7 standard deviations above it.

References

[1] Particle Data Group, E. Phys. J. **C15** (2000) 1-878

[2] L. Bertanza *et al.*, Z. Phys. **C73** (1997) 629-632.

[3] L. K. Gibbons *et al.*, Phys. Rev. Lett. **70** (1993) 1199-1202.

[4] B. Schwingenheuer *et al.*, Phys. Rev. Lett. **74** (1995) 4376-4379.

[5] A. Lai *et al.*, E. Phys. J. **C22** (2001) 231-254.

[6] C. Biino *et al.*, CERN-SL-98-033 (EA) and Proceedings of the 6th EPAC, Stockholm 1998, IoP, 2100-2102 (1999).

[7] D. Béderède *et al.*, Nucl. Inst. Meth. **A367** (1995) 88-91;
     I. Augustin *et al.*, Nucl. Inst. Meth. **A403** (1998) 472-480.

[8] G. D. Barr *et al.*, Nucl. Inst. Meth. **A370** (1996) 413-424;
     B. Hallgren *et al.*, Nucl. Inst. Meth. **A419** (1998) 680-685;
     G. Unal for the NA48 Collaboration, 9th International Conference on Calorimetry, October 2000, Annecy, France, hep-ex/0012011.

[9] G. D. Barr *et al.*, "The trigger for $K^0 \to \pi^0\pi^0$ decays of the NA48 experiment at CERN", CERN-EP/2001-079 (Nov. 2001), to be published in Nucl. Inst. Meth..

[10] S. Anvar *et al.*, Nucl. Inst. Meth. **A419** (1998) 686-694.

[11] H. Bergauer *et al.*, Nucl. Inst. Meth. **A419** (1998) 623-631.

[12] GEANT Detector Description and Simulation Tool, CERN Program Library Long Write-up W5013 (1994).

[13] R. Carosi *et al.*, Phys. Lett. **B237** (1990) 303-312.

[14] The collimator scattering background fraction of $(9.6 \pm 2.0) \times 10^{-4}$ determined in ref. [5] refers to K_L decays which have been weighted according to their reconstructed proper lifetime.